I J R B A T, Issue (XIII) Volume (II) May 2025: 100-113 OPEN ACCESS e-ISSN 2347 – 517X
A Double-Blind Peer Reviewed & Refereed Journal Original Article

INTERNATIONAL JOURNAL OF RESEARCHES IN BIOSCIENCES, AGRICULTURE AND TECHNOLOGY

 www.ijrbat.in

STABILITY OF RUBANS ANISOTROPIC COSMOLOGICAL MODEL IN BRANS-DICKE THEORY OF GRAVITATION

Nimkar H. A., Ugale M.R.*, Dhore A.O.**

Department of Applied Science and Humanities
Dr. Rajendra Gode Institute of Technology and Research, Amravati, M.S. India
*Department of Science and Humanities
Sipna College of Engineering and Technology, Amravati, M.S. India
**Department of Mathematics
Shri. Dr. R. G. Rathod Arts and Science College, Murtizapur, Akola, M.S. India
Email: harshalnimkar53@gmail.com , mrugale@sipnaengg.ac.in, drabhijeetdhore@gmail.com

Communicated: 28.11.2024 Revision: 17.01.2025 & 29.01.2025 Accepted: 28.02.2025 Published: 31.05.2025

ABSTRACT:

In this paper, a detailed investigation of the stability of Ruban space-time, an anisotropic cosmological model in the framework of the Brans-Dicke theory of gravitation, with a specific focus on the influence of anisotropic dark matter *(DM)* distribution. The Ruban space-time, being an inhomogeneous generalization of the Szekeres model, is adopted as the geometric background. We solve the Brans-Dicke field equations by assuming a trace-free energy-momentum tensor and adopting a linear variation law of the deceleration parameter, which facilitates a constant deceleration scenario. Furthermore, proportionality between the shear scalar and the expansion scalar is imposed to reduce the complexity of the field equations and obtained exact solutions.

We derive cosmological parameters such as the Hubble parameter, deceleration parameter, expansion scalar, shear scalar, anisotropy parameter, energy density and transverse pressure and radial pressure, which are expressed as functions of redshift, allowing a comprehensive study of the model's dynamical behavior. Also examine the stability with the help of the square of sound speed relation and causality condition. energy conditions, including Null, Weak, and Strong Energy Conditions. Additionally, the model is confronted with recent Hubble observational datasets comprising 57 data points over a wide redshift range, incorporating both differential age and baryon acoustic oscillation *(BAO)* methods. Best-fit parameters are obtained through curve fitting techniques, yielding a low root mean square error *(RMSE)* and high correlation, thereby demonstrating consistency with observational data. Om-diagnostics, which validate the model's ability to replicate dark energy-like behavior under scalar-tensor theory, provide more evidence for the model's feasibility.

In conclusion, the proposed Ruban Brans-Dicke anisotropic cosmological model with dark matter content offers a stable, observationally consistent framework for explaining the universe's expansion dynamics, particularly in the presence of anisotropic pressures and varying gravitational coupling.

Keywords: Ruban, Brans – Dicke Theory, anisotropic dark matter.

INTRODUCTION:

The theory of general relativity is one of the best theories of gravitational interaction. Even though its predictions were examined with extremely high precision, there remain unanswered issues due to which general relativity gets modified. The Brans-Dicke theory of gravity is one of the most important scalar-tensor theories of gravity due to its vast cosmological implications. The latest inflationary models possible "graceful exit" problem and extended chaotic inflations are based on Brans-Dicke scalar-tensor theory. The Brans-Dicke theory of gravity (1961) is one of the simplest extensions of general relativity, depending on one additional parameter ω . In addition to the metric, the gravitational field is further mediated by a scalar field ϕ whose inverse plays the role of a space-time-varying gravitational strength. Brans-Dicke

http://doi.org/10.29369/ijrbat.2025.010.2.00012

theory is a generalization of general relativity which is more consistent with Mach's principle and involves a violation

of the strong principle of equivalence, but the weak principle of equivalence is satisfied. A dynamical scalar field ϕ is introduced in Brans-Dicke which corresponds to the variation in gravitational constant with respect to cosmic time, i.e. $\phi \approx G^{-1}$ and coupled to gravity with coupling parameter ω

Brans- Dicke field equations for combined scalar and tensor fields are

$$G_{ij} = -8\pi\phi^{-1}T_{ij} - \omega\phi^{-2}\left(\phi_{,i}\phi_{,j} - \frac{1}{2}g_{ij}\phi_{,k}\phi^{,k}\right) - \phi^{-1}\left(\phi_{i;j} - g_{ij}\phi^{,k}_{,k}\right) \quad (1)$$

And

$$\phi = \phi^{,k}_{,k} = \frac{8\pi\phi^{-1}T}{(3+2\omega)} \quad (2)$$

Where, $G_{ij} = R_{ij} - \frac{1}{2}g_{ij}R$ is an Einstein tensor, T_{ij} is the stress-energy tensor of the matter, ω is the dimensionless coupling constant, comma and semicolons denote partial and covariant differentiation, respectively. Many authors have discussed several aspects of Brans-Dicke theory viz., Ahmadi Azar et al. (2024), Mishra et al. (2024), Sharma et al. (2025), Vijaya Santhi et al. (2024), Satyanarayana et al. (2024), Halife Caglar (2023), Bamba et al. (2023), Vijaya Santhi et al. (2022), Bhardwaj et al.(2023), Kapse et al. (2022), Roy (2021), Singh et al. (2021), Shaikh (2020), Aditya et al. (2019), Pawar et al. (2018), Tirandari et al. (2017), Biswas et al. (2014), Pawar et al. (2014), Avilez et al. (2014), Vidya Sager et al. (2014), Reddy et al. (2014), Adhav et al. (2008).

There are few studies in the literature about Ruban universe model. Lima et al. (1990) have investigated the solutions of Ruban universe model with electromagnetic field. Lima et al. (1988) have studied inhomogeneous two cosmological models. Tomimura et al. (1987) have obtained exact solutions of Ruban space-time with dust, radiation and electromagnetic field. Recently, Wath et al. (2024) have examined the Stability of macroscopic body cosmological model in Ruban's background. Aktas (2019) studied energy momentum distributions of Ruban universe in general relativity and teleparallel gravity. Mete et al. (2015) have investigated Ruban's cosmological model in presence of bulk stress source in the framework of general theory of relativity.

The discovery of invisible matter called dark matter. Dark matter plays an important role in the formation of galaxies. Many researchers have been theoretically and experimentally attracted to the nature of

dark matter. Ugale et al. (2024), Dhore et al. (2024), Nayan Sarkar et al. (2020), Piyali Bhar et al. (2017), wath et al. (2024) are some of the authors who have obtained cosmological model for an anisotropic dark matter distribution the energy momentum tensor.

In addition to this, Wath et al. (2023), Thirukkanesh et al. (2021), Herrera (2020), Ahmed et al. (2018), Franco et al. (2020), Knutsen (1988), wanas et al. (1995) have analysed stability of cosmological model using various Method.

Motivated by the above discussion and observed facts, in the present paper, we propose to study Ruban Cosmological model in the presence of an anisotropic dark matter distribution. Our paper is organized as follows. In section 2 Metric and field equations. In Section 3 Solutions of the field equations. In Section 4 contains Physical and Kinematical properties of the model. Section 5 contains Stability analysis; Section 6 contains Hubble Data and Energy Conditions. The last Section contains some conclusions.

2 Metric and Field Equations

As everyone knows, models of the universe, such as the inhomogeneous and anisotropic Szekeres metrics, are critical for understanding how the universe originated. The Ruban universe model is also a variant of the Szekeres universe. It is not homogeneous and not the same everywhere. Ruban's model of space- time is given by (1990)

$$ds^2 = dt^2 - Q^2(x,t)dx^2 - R^2(t)\left(dy^2 + h^2dz^2\right)$$

http://doi.org/10.29369/ijrbat.2025.010.2.00012

Where, $h(y)=\frac{\sin\sqrt{k}y}{\sqrt{k}}=\begin{matrix}\sin y\ if\ k=1\\ y\ \ if\ k=0\\ \sinh y\ if\ k=-1\end{matrix}$ (3)

and k is the curvature parameter of the homogeneous 2-spaces t and x constants. The functions Q and R are free and will be determined.

For an anisotropic DM matter distribution, the energy momentum can be written as

$$T_{ij}=(\rho+p_t)u_iu_j-p_tg_{ij}+(p_r-p_t)\chi_i\chi_j \quad (4)$$

where $\rho=\rho(r)$, $p_r=p_r(r)$ and $p_t=p_t(r)$ stand for the energy density, radial pressure and transverse pressure of fluid sphere respectively $u^iu_i=-\chi^i\chi_i=1$ and $u^i\chi_i=0$, u^i is the four velocity vector of the particles and χ^i is the direction of anisotropy.

From equation (4), we have

$$T_1^1=-p_r,\ T_2^2=T_3^3=-p_t \text{ and } T_4^4=\rho \quad (5)$$

Using the equations (1), (2), (4) and (5), the field equations of metric (3) are

$$2\frac{\ddot{R}}{R}+\frac{\dot{R}^2}{R^2}+\frac{k}{R^2}+\frac{\omega}{2}\frac{\dot{\phi}^2}{\phi^2}+2\frac{\dot{R}}{R}\frac{\dot{\phi}}{\phi}+\frac{\ddot{\phi}}{\phi}=-8\pi\phi^{-1}p_r \quad (6)$$

$$\frac{\dot{R}\dot{Q}}{RQ}+\frac{\ddot{R}}{R}+\frac{\ddot{Q}}{Q}+\frac{\omega}{2}\frac{\dot{\phi}^2}{\phi^2}+\left(\frac{\dot{Q}}{Q}+\frac{\dot{R}}{R}\right)\frac{\dot{\phi}}{\phi}+\frac{\ddot{\phi}}{\phi}=-8\pi\phi^{-1}p_t \quad (7)$$

$$2\frac{\dot{R}\dot{Q}}{RQ}+\frac{\dot{R}^2}{R^2}+\frac{k}{R^2}-\frac{\omega}{2}\frac{\dot{\phi}^2}{\phi^2}+\left(\frac{\dot{Q}}{Q}+2\frac{\dot{R}}{R}\right)\frac{\dot{\phi}}{\phi}=8\pi\phi^{-1}\rho \quad (8)$$

$$\ddot{\phi}+\left(\frac{\dot{Q}}{Q}+2\frac{\dot{R}}{R}\right)\phi_4=\frac{8\pi\phi^{-1}}{(3+2\omega)}T \quad (9)$$

Here over head dot denotes ordinary differentiation with respect to time t.

The anisotropic factor is defined as $\Delta(r)=p_t(r)-p_r(r)$. The radial and transverse equation of parameters are defined as $\omega_r(r)=\frac{p_r(r)}{\rho(r)}$ and $\omega_t(r)=\frac{p_t(r)}{\rho(r)}$, these two are most important tool in the study of anisotropic matter configuration and they satisfy the condition $0<\omega_r(r),\ \omega_t(r)<1$ for physical matter distribution (2010).

For Rubans cosmological model, the average scale factor $a(t)$ and spatial volume V are given by

$$a(t)=(QR^2h)^{\frac{1}{3}} \quad (10)$$

$$V=a^3(t)=(QR^2h) \quad (11)$$

The mean generalized Hubble parameter H for this model is given by

$$H=\frac{1}{3}\left(\frac{\dot{Q}}{Q}+2\frac{\dot{R}}{R}\right) \quad (12)$$

where H_1,H_2,H_3 are the directional Hubble parameters defined by

$$H_1=\frac{\dot{Q}}{Q},H_2=H_3=\frac{\dot{R}}{R} \quad (13)$$

The average anisotropy parameter is

$$A_m=\frac{1}{3}\sum_{i=1}^{3}\left(\frac{\Delta H_i}{H}\right)$$

where $\Delta H_i=H_i-H$. The expansion Scalar θ and shear scalar σ are given by

$$\theta=3H=\left(\frac{\dot{Q}}{Q}+2\frac{\dot{R}}{R}\right) \quad (14)$$

$$\sigma^2=\frac{3}{2}A_mH^2=\frac{1}{3}\left[\frac{\dot{Q}}{Q}-\frac{\dot{R}}{R}\right]^2 \quad (15)$$

3 Solutions of Field Equations

The field equations (6) - (9) are four equations in six unknowns R,Q,ϕ,p_t,p_r and ρ they are highly nonlinear differential equation, so that we need some extra constraints. Hence, to find a determinate solution, we use the following

http://doi.org/10.29369/ijrbat.2025.010.2.00012

conditions, which physically corresponds the vanishing of trace of an anisotropic dark matter. This is analogous to the disordered radiation condition of general relativity by M. Kiran (2015).

$$T = \rho - p_r - 2p_t = 0 \qquad (16)$$

Also, we use the condition that the shear scalar σ is directly proportional to expansion scalar θ.

$$\sigma \propto \theta \Rightarrow \sigma = k_1\theta \qquad (17)$$

Where, k_1 is proportionality constant, Using equations (14) and (15), equation (17) becomes,

$$\frac{1}{\sqrt{3}}\left(\frac{\dot{Q}}{Q} - \frac{\dot{R}}{R}\right) = k_1\left(\frac{\dot{Q}}{Q} + 2\frac{\dot{R}}{R}\right) \qquad (18)$$

On integrating equation (18) we get,

$$Q = R^{\frac{2\sqrt{3}k_1+1}{1-\sqrt{3}k_1}} \qquad (19)$$

Now, we consider a generalized linearly varying deceleration parameter Akarsu and Dereli (2012)

$$q = \frac{-a\ddot{a}}{\dot{a}^2} \qquad (20)$$

The rate of expansion of the universe is measured by the deceleration parameter. The sign of q indicates that the universe is expanding. Where $q > 0$ denotes deflection and $q < 0$ indicates inflation. However, expansion with constant velocity is shown at $q = 0$ Berman (1983), Berman and Gomide (1988), proposed a law of variation for the Hubble parameter in the context of FLRW (Friedmann Lemaitre- Robertson-walker) space-time in GR. (General Relativity). This led to a constant deceleration parameter ($q = n-1, n \geq 0$). Following the discovery of the present acceleration of the universe, Several writers have examined cosmological models utilizing Berman's law in the context of DE. This is because the deceleration parameter in Berman's law can have values $q \geq -1$ and $-1 \leq q < 0$ corresponding to the linearly deceleration parameter (2012), which is given by

$$q = -k_2 t + n - 1 \qquad (21)$$

Where, $k_2 \geq 0$ and $n \geq 0$ are constants, $k_2 = 0$ equation (21) reduces to the law of Berman (1988) this law allows for the generalization of constant deceleration parameter- derived cosmological solutions. Our linearly varying deceleration parameter approach leads to the universe undergoing super exponential expansion unless $k_2 = 0$, which is one of the conceivable outcomes of the universe based on cosmological evidence. From eq.(20) and (21),we get the value of the average scale factor as

$$a = k_3(nt + k_4)^{\frac{1}{n}} \qquad (22)$$

for $k_2 = 0 \,\&\, n > 0$ where k_3, k_4 are constant of integration.

From equation (11), (19) and (22) we get,

$$R = k_5(nt + k_4)^{\frac{1-\sqrt{3}k_1}{n}} \qquad (23)$$

$$Q = k_6(nt + k_4)^{\frac{2\sqrt{3}k_1+1}{n}} \qquad (24)$$

where, $k_5 = k_3^{(1-\sqrt{3}k_1)}$, $k_6 = k_5^{\frac{2\sqrt{3}k_1+1}{1-\sqrt{3}k_1}}$

By using equations (23) and (24), equation (3) takes the form

$$ds^2 = dt^2 - \left[k_6(nt + k_4)^{\frac{2\sqrt{3}k_1+1}{n}}\right]^2 dx^2 - \left[k_5(nt + k_4)^{\frac{1-\sqrt{3}k_1}{n}}\right]^2 \left(dy^2 + hdz^2\right) \qquad (25)$$

4 Physical and Kinematical properties of the model:

Redshift is a highly significant and often contentious phenomenon regarding cosmology and astronomy. When electromagnetic radiation from an object is directed towards the less energetic regions of the spectrum, a phenomenon known as the shift in electromagnetic radiation occurs. Utilizing this phenomenon to get insight into aspects of our galaxy and even the whole universe. The relation between average scale factor a redshift z (2023) is

http://doi.org/10.29369/ijrbat.2025.010.2.00012

$$a = \frac{1}{1+z} \qquad (26)$$

In this section, we have estimated and determined significant cosmological quantities in connection to redshift. These computations aid our understanding of the expansion of the universe, energy distribution and the effects of many components at various redshifts. The key cosmological parameters, deceleration parameter (q), Hubble parameter (H), anisotropy parameter (A_m), expansion scalar (θ) and shear scalar (σ^2) in terms of redshift are calculated as

$$q = -1 - \frac{k_2 k_3^n}{n(1+z)^n} + k_2 k_4 + n \qquad (27)$$

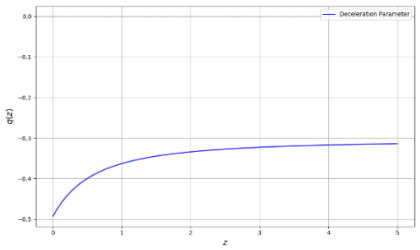

Fig.1 Plot Deceleration parameter (q) versus redshift (z) for

$$n = 1.695, k_2 = 10, k_3 = 0.131, k_4 = -0.1$$

A positive sign of the deceleration parameter q indicates the standard decelerating model, whereas the negative sign indicates the inflating model. Recent observation shows that the deceleration parameter of the range of $-1 < q < 0$ and present day universe is undergoing an accelerated expansion. From fig.1, it is observed that deceleration parameter q is in the range (-1, 0) hence, the model represents accelerated expansion of the universe.

$$H = \frac{(1+z)^n}{k_3^n} \qquad (28)$$

$$\theta = \frac{3(1+z)^n}{k_3^n} \qquad (29)$$

$$\sigma^2 = \frac{9k_1^2(1+z)^{2n}}{k_3^{2n}} \qquad (30)$$

$$A_m = 6k_1^2 \qquad (31)$$

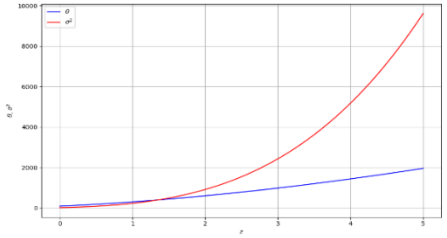

Fig.2 Plot expansion scalar (θ) and shear scalar (σ^2) versus redshift (z) for

$$n = 1.695, k_1 = 0.05, k_3 = 0.131$$

From fig.2 it is observed that both expansion scalar and shear scalar increases as redshift increases, whereas when redshift is zero, the expansion scalar and shear scalars are finite.

Solving equation (9) by using equations (16), (23) and (24), we obtained scale factor in terms of redshift.

$$\phi = \frac{k_{10}}{(1+z)^{(n-3)}} \qquad (32)$$

The expressions for transverse pressure (p_t), radial pressure (p_r), energy density (ρ), and anisotropic factor

(Δr) are obtained in the following form

$$p_t = \frac{-k_9}{8\pi}\left[\frac{k_{10}(1+z)^{(n+3)}}{k_3^{(n+3)}} + \frac{k_{13}(1+z)^{(n+3)}}{k_3^{(n+3)}} + \frac{k_{14}(1+z)^{(n+3)}}{k_3^{(n+3)}} + \frac{\omega(n-3)^2(1+z)^{(n+3)}}{k_3^{(n+3)}}\right]$$

33)

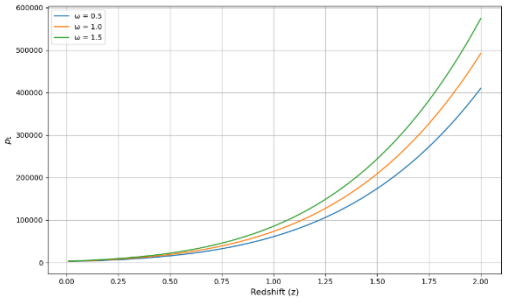

Fig.3 Plot transverse pressure (p_t) versus redshift (z) for

$$n = 1.695, k_3 = 0.131, k_9 = -1, k_{10} = 1, k_{13} = k_{14} = 1.2$$

$$p_r = \frac{-k_9}{8\pi}\left[\frac{2k_{10}(1+z)^{(n+3)}}{k_3^{(n+3)}} + \frac{k(1+z)^{(4-\sqrt{3}k_1+n)}}{k_5^2 k_3^{(4-\sqrt{3}k_1+n)}} + \frac{\omega(n-3)^2(1+z)^{(n+3)}}{2k_3^{(n+3)}} + \frac{k_{12}(1+z)^{(n+3)}}{k_3^{(n+3)}}\right]$$

(34)

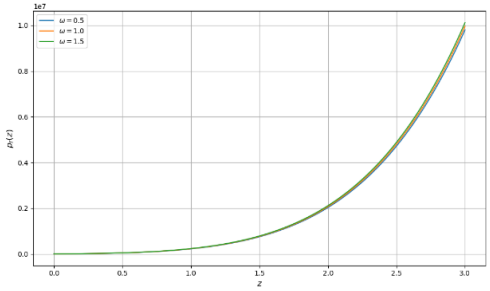

http://doi.org/10.29369/ijrbat.2025.010.2.00012

Fig.4 Plot radial pressure (p_r) versus redshift (z) for $n=1.695, k=1, k_1=0.05, k_3=0.131, k_5=1.5, k_9=-1, k_{10}=k_{12}=1$

$$\rho=\frac{k_9}{8\pi}\left[\frac{2k_{10}(1+z)^{(n+3)}}{k_3^{(n+3)}}+\frac{\left(1-\sqrt{3}k_1\right)^2(1+z)^{(n+3)}}{k_3^{(n+3)}}+\frac{kk_3^{nk_{11}}}{k_5^2(1+z)^{nk_{11}}}-\frac{\omega(n-3)^2(1+z)^{(n+3)}}{2k_3^{(n+3)}}+\frac{3(n-3)(1+z)^{(n+3)}}{k_3^{(n+3)}}\right]$$

(35)

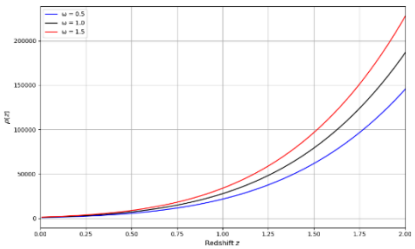

Fig.5 Plot energy density (ρ) versus redshift (z) for $n=1.695, k=1, k_1=0.05, k_3=0.131, k_5=1.5, k_9=-1, k_{10}=1, k_{11}=0.5$

From fig.3, fig.4, and fig.5, we can observe that the curve of transverse pressure, radial pressure and energy density are varying in positive region throughout the evolution of the universe against redshift, which indicates that the universe is expanding.

$$\Delta(r)=\frac{k_9}{8\pi}\left[\frac{k_{10}(1+z)^{(n+3)}}{k_3^{(n+3)}}-\frac{k_{13}(1+z)^{(n+3)}}{k_3^{(n+3)}}-\frac{k_{14}(1+z)^{(n+3)}}{k_3^{(n+3)}}-\frac{\omega(n-2)^2(1+z)^{(n+3)}}{2k_3^{(n+3)}}+\frac{k(1+z)^{\left(4-\sqrt{3}k_1+n\right)}}{k_5^2k_3^{\left(4-\sqrt{3}k_1+n\right)}}\right.$$
$$\left.+\frac{k(1+z)^{\left(4-\sqrt{3}k_1+n\right)}}{k_5^2k_3^{\left(4-\sqrt{3}k_1+n\right)}}+\frac{\omega(n-3)^2(1+z)^{(n+3)}}{k_3^{n+3}}+\frac{k_{12}(1+z)}{k_3^{(n+3)}}\right]$$

(36)

5 Stability Analyses

Using different aspects we discuss the stability of the model.

Speed of Sound

The physical quantities $v_r^2=\frac{dp_r(r)}{d\rho(r)}$ and $v_t^2=\frac{dp_t(r)}{d\rho(r)}$ describing the behaviour of radial and tangential sound speeds respectively. When both the ratios are positive, i.e. $v_r^2>0$ and $v_t^2>0$, we have a stable model whereas when both the ratios are negative, i.e. $v_r^2<0$ and $v_t^2<0$, we have an unstable model. From equation (33) to equation (35) we get,

$$v_r^2=\frac{dp_r(r)}{d\rho(r)}=\left[\frac{k_5^2(1+z)^{nk_{11}+1}}{nkk_{11}k_3^{nk_{11}}}-\frac{k_{12}}{3(n-3)}-\frac{k\left(4-\sqrt{3}k_1+n\right)(1+z)^{\left(3-\sqrt{3}k_1+n\right)}k_3^{(n+3)}}{k_5^2k_3^{\left(4-\sqrt{3}k_1+n\right)}\left(1-\sqrt{3}k_1\right)^2(n+3)(1+z)^{(n+2)}}\right] \quad (37)$$

$$v_t^2=\frac{dp_t(r)}{d\rho(r)}=\left[\frac{k_{14}(n+3)(1+z)^{n+2}k_5^2(1+z)^{nk_{11}+1}}{nkk_{11}k_3^{(n+3)}k_3^{nk_{11}}}+\frac{(n+2)^2}{2(n-3)^2}-\frac{k_3^{(n+3)}}{3\left(n^2-9\right)(1+z)^{(n+2)}}-\frac{k_{13}}{\left(1-\sqrt{3}k_1\right)^2}-\frac{1}{2}\right]$$

(38)

In these model, it is observed that both the ratios are positive, i.e. $v_r^2>0$ and $v_t^2>0$. So the given cosmological model is stable.

The causality condition

In addition to the positivity of v_r^2 and v_t^2, the causality condition states that the speed of sound is less than the speed of light and can be describe as

$$0\le v_r=\sqrt{\frac{dp_r(r)}{d\rho(r)}}\le 1 \quad \text{and}$$
$$0\le v_t=\sqrt{\frac{dp_t(r)}{d\rho(r)}}\le 1$$

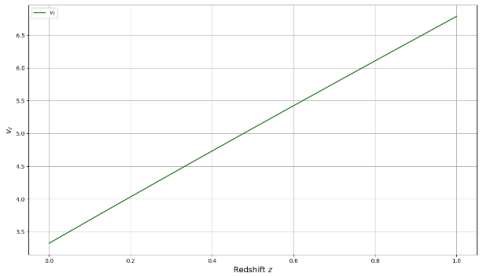

http://doi.org/10.29369/ijrbat.2025.010.2.00012

Fig.6 Plot of radial velocity (v_r) versus redshift (z) for $n=1.695, k=1, k_1=0.05, k_3=0.131, k_5=1.5, k_{11}=0.5=k_{12}=1$

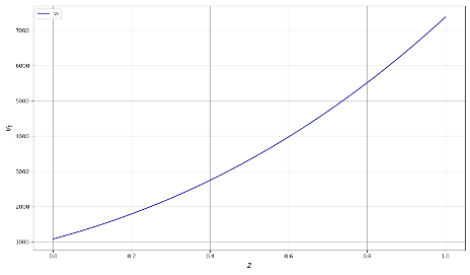

Fig.7 Plot of transverse velocity (v_t) versus redshift (z) for $n=1.695, k=1, k_1=0.05, k_3=0.131, k_5=1.5, k_{11}=0.5, k_{13}=1, k_{14}=2$

In the given cosmological model, the speed of sound is greater than one, but the speed of sound is not less than the speed of light, i.e., it does not lie between 0 and 1. So, the causality condition is not satisfied.

The stability condition

To study the stability Sarkar et al. (2020) and Abreu et al. (2007) provides the conditions with respect to the stability factor $\left(v_t^2 - v_r^2\right)$ for an anisotropic fluid model. The stability condition is described as from equation (37) and equation (38) we obtained,

$$\left(v_t^2 - v_r^2\right) = \left[\left(\frac{k_{14}(n+3)(1+z)^{(n+2)}}{k_3^{(n+3)}} - 1\right)\frac{k_5^2(1+z)^{nk_{11}+1}}{nkk_{11}k_3^{nk_{11}}} + \frac{(n+2)^2}{2(n-3)^2} - \frac{k_3^{(n+3)}}{3(n^2-9)(1+z)^{(n+3)}} - \frac{k_{13}}{\left(1-\sqrt{3}k_1\right)^2} - \frac{1}{2} + \frac{k_{12}}{3(n-3)} + \frac{k\left(4-\sqrt{3}k_1+n\right)(1+z)^{\left(3-\sqrt{3}k_1+n\right)}}{k_5^2 k_3^{\left(4-\sqrt{3}k_1+n\right)}\left(1-\sqrt{3}k_1\right)^2(n+3)(1+z)^{(n+3)}}\right] \quad (39)$$

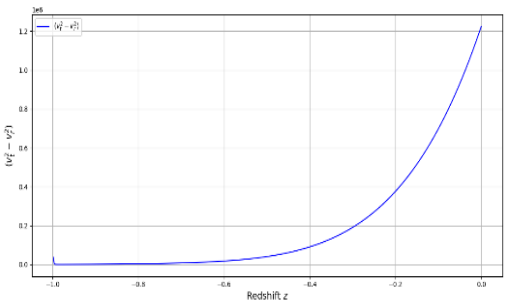

Fig.8 Plot of stability factor $\left(v_t^2 - v_r^2\right)$ versus redshift (z) for $n=1.695, k=1, k_1=0.05, k_3=0.131, k_5=1.5, k_{11}=0.5, k_{12}=1=k_{13}$

The region is potentially stable if $-1<\left(v_t^2 - v_r^2\right)<0$ and the region is potentially unstable if $0<\left(v_t^2 - v_r^2\right)<1$. From fig. 8 it is clear that stability factor $\left(v_t^2 - v_r^2\right)$ lies between (-1 0). So, the model is stable.

6 Hubble Datasets

Measurement of dt yields the Hubble parameter, which is independent of the model, as the Hubble parameter is also related to the differential redshift, as $H(z) = -\frac{1}{(1+z)}\frac{dz}{dt}$ where dz is acquired from the spectroscopic surveys. Actually, there are two common approaches to determining the Hubble parameter values $H(z)$ at a given redshift: a differential age (DA) and the line-of-sight baryonic acoustic oscillation (BAO) datasets. The 57 newest $H(z)$ data points in the redshift range of $0.070 \le z \le 2.36$ provide observational constraints on parameters $H_0 = \in(\lambda+1)$. The DA technique was used to collect 31 points, and the BAO technique was used to collect 26 points. A list of 57 $H(z)$ values in the redshift range $0.070 \le z \le 2.36$ has been proposed in (2018 & 2020) (see Table 1). We found the best-fit curve of $H(z)$ with 57 data values shown in Table 1, using the $R^2 - test$:

http 2.00012

$$R^2 = 1 - \frac{\sum_{i=1}^{57}\left[(H_i)_{obs} - (H_i)_{th}\right]^2}{\sum_{i=1}^{57}\left[(H_i)_{obs} - (H_i)_{mean}\right]^2} \quad (40)$$

The $R^2 - test$ examines how much of the universe in the dependent variable can be explained by the independent variable. Regarding the values of model parameters H_0, δ and λ in relation to the observatory Hubble dataset (HOD), a $R^2 = 1$ denotes an exact fit. To determine the optimal values of H_0, δ and λ, we limit the parametric spaces $-1 < z$ and $\in \neq 0$. For $H_0 = 67.8 kms^{-1}Mpc^{-1}$, $\Omega_m = 0.3$ and $\Omega_\Lambda = 0.7$, the error bars show the mean point and how far it is from the mean across 57 points of the Hubble dataset $H(z) = H_0\sqrt{\Omega_m(1+z)^3 + \Omega_\Lambda}$. Here, Ω_m and Ω_Λ are the density parameters of dark matter dark energy, respectively. For appximate values of $H_0 = 64.49^{+0.33}_{-0.32}, n = 1.695, k_3 = 0.131$ we obtain the best-fit plot with a maximum of $R^2 = 0.9321$ and a root mean square error (RMSE) of 11.071.

z	$H(z)$	σ_H	Ref.	z	$H(z)$	σ_H	Ref.
0.070	69	19.6	Stern et al. (2010)	1.750	202	40	Simon et al. (2005)
0.90	69	12	Simon et al. (2005)	1.965	186.5	50.4	Moresco (2015)
0.120	68.6	26.2	Stern et al. (2010)	0.24	79.69	2.99	Gaztanaga et al. (2009)
0.170	83	8	Simon et al. (2005)	0.30	81.7	6.22	Oka et al. (2014)
0.1791	75	4	Moresco et al. (2012)	0.31	78.18	4.74	Wang et al. (2017)
0.1993	75	5	Moresco et al. (2012)	0.34	83.8	3.66	Gaztanaga et al. (2009)
0.200	72.9	29.6	Zhang et al. (2014)	0.35	82.7	9.1	Ratsimbazafy et al. (2016)
0.270	77	14	Simon et al. (2005)	0.36	79.94	3.38	Wang et al. (2017)
0.280	88.8	36.6	Zhang et al. (2014)	0.38	81.5	1.9	Alam et al. (2017)
0.3519	83	14	Moresco et al. (2012)	0.40	82.04	2.03	Wang et al. (2017)
0.3802	83	13.5	Moresco et al. (2016)	0.43	86.45	3.97	Gaztanaga et al. (2009)
0400	95	17	Simon et al. (2005)	0.44	82.6	7.8	Blake et al. (2012)
0.4004	77	10.2	Moresco et al. (2016)	0.44	84.84	1.83	Wang et al. (2017)
0.4247	87.1	11.2	Moresco et al. (2016)	0.48	87.79	2.03	Wang et al. (2017)
0.4497	92.8	12.9	Moresco et al. (2016)	0.51	90.4	1.9	Wang et al. (2017)
0.470	89	34	Ratsimbazafy et al. (2017)	0.52	94.35	2.64	Wang et al. (2017)
0.4783	80.9	9	Moresco et al. (2016)	0.56	93.34	2.3	Wang et al. (2017)
0.480	97	62	Stern et al. (2010)	0.57	87.6	7.8	Chuang et al. (2013)
0.593	104	13	Moresco et al. (2012)	0.57	96.8	3.4	Anderson et al. (2014)
0.6797	92	8	Moresco et al. (2012)	0.59	98.48	3.18	Wang et al. (2017)
0.7812	105	12	Moresco et al. (2012)	0.60	87.9	6.1	Blake et al. (2012)
0.8754	125	17	Moresco et al. (2012)	0.61	97.3	2.1	Alam et al. (2017)
0.880	90	40	Stern et al. (2010)	0.64	98.82	2.98	Wang et al. (2017)
0.900	117	23	Simon et al. (2005)	0.73	97.3	7.0	Blake et al. (2012)
1.037	154	20	Moresco et al. (2012)	2.30	224	8.6	Delubac et al. (2012)
1.300	168	17	Simon et al. (2005)	2.33	224	8	Bautista et al. (2017)
1.363	160	33.6	Moresco (2015)	2.34	222	8.5	Delubac et al. (2013)
1.430	177	18	Simon et al. (2005)	2.26	226	9.3	Font-Ribera et al. (2014)
1.530	140	14	Simon et al. (2005)				

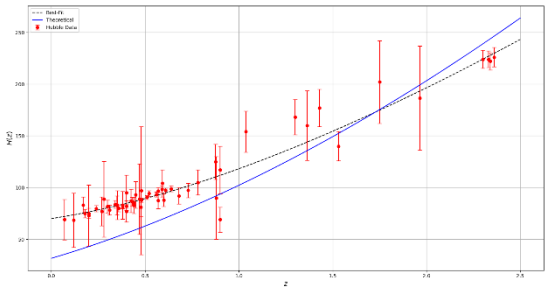

http://doi.org/10.29369/ijrbat.2025.010.2.00012

Fig.5 Plot Hubble Data versus redshift along with Hubble data set given in Table 1

From fig. (5) It is observed that best-fitted curve closely matched the data points when we compared the graph of the Hubble parameter with the Hubble dataset. The graph illustrates the history of the expansion of the universe, which is characterized by an increase in the Hubble parameter as redshift increases. The universe underwent a transition from early-time decelerated expansion to late-time accelerated expansion. The best-fit line aligns well with observational data, while the theoretical model slightly over predicts H(z) at higher redshifts. This suggests the theoretical model captures the general expansion behavior but may need refinement. Overall, the universe's expansion history supports the standard cosmological model with evolving dynamics over cosmic time.

7 Energy Conditions

Energy conditions are sets of mathematical inequalities imposed on the energy-momentum tensor T_{ij}, which describe the matter and energy content of the universe in the framework of general relativity. These conditions provide a way to ensure the physical viability of a cosmological model and impose constraints on the behavior of matter and energy under gravitational interactions.

1. **Null Energy Condition (NEC):** The Null Energy Condition requires $\rho + p \geq 0$. The NEC ensures that the energy density observed by a light-like observer (null vector) is non-negative. It is the most fundamental of all energy conditions, as the violation of the NEC often leads to unphysical scenarios such as exotic matter or superluminal signals. In an expanding universe, the NEC is closely linked to the second law of thermodynamics and the avoidance of unphysical singularities.
2. **Weak Energy Condition (WEC):** the weak energy condition requires $\rho \geq 0, \rho + p \geq 0.$ The WEC ensures that the energy density observed by any time like observer is non-negative. This condition is fundamental for a physically reasonable distribution of matter and energy. Satisfying the WEC indicates that matter behaves normally (e.g., no negative energy densities). It guarantees the normal gravitational attraction of matter and aligns with the observed dynamics of galaxies and cosmic structures.
3. **Strong Energy Condition (SEC):** The Strong Energy Condition requires $\rho + 3p \geq 0,$ $\rho + p \geq 0.$ The SEC ensure that gravity is always attractive, implying that the combined effects of energy density and pressure act as a source of gravitational pull. The SEC is rooted in classical general relativity, where gravity is inherently attractive. In standard cosmology, the SEC is satisfied during the matter-dominated and radiation-dominated phases. However, during the accelerated expansion of the universe (e.g., the inflationary epoch or the current dark energy-dominated era), the SEC is violated. This violation is necessary to explain repulsive gravitational effects, such as the ones driving the universe's accelerated expansion.

For our model in terms of redshift, we obtain

$$\rho(z)+p_r(z)=\frac{k_9}{8\pi}\left[\frac{\left(1-\sqrt{3}k_1\right)^2(1+z)^{(n+3)}}{k_3^{(n+3)}}+\frac{kk_3^{nk_{11}}}{k_5^2(1+z)^{nk_{11}}}-\frac{\omega(n-3)^2(1+z)^{(n+3)}}{k_3^{(n+3)}}+\frac{3(n-3)(1+z)^{(n+3)}}{k_3^{(n+3)}}-\frac{k(1+z)^{\left(4-\sqrt{3}k_1+n\right)}}{k_5^2k_3^{\left(4-\sqrt{3}k_1+n\right)}}-\frac{k_{12}(1+z)^{(n+3)}}{k_3^{(n+3)}}\right] \quad (41)$$

$$\rho(z)+p_t(z)=\frac{k_9}{8\pi}\left[\frac{k_{10}(1+z)^{(n+3)}}{k_3^{(n+3)}}+\frac{\left(1-\sqrt{3}k_1\right)^2(1+z)^{(n+3)}}{k_3^{(n+3)}}+\frac{kk_3^{nk_{11}}}{k_5^2(1+z)^{nk_{11}}}-\frac{\omega(n-3)^2(1+z)^{(n+3)}}{k_3^{(n+3)}}+\frac{3(n-3)(1+z)^{(n+3)}}{k_3^{(n+3)}}-\frac{k_{13}(1+z)^{(n+3)}}{k_3^{(n+3)}}-\frac{k_{14}(1+z)^{(n+3)}}{k_3^{(n+3)}}\right] \quad (42)$$

http://doi.org/10.29369/ijrbat.2025.010.2.00012

$$\rho(z)-p_r(z)=\frac{k_9}{8\pi}\left[\frac{4k_{10}(1+z)^{(n+3)}}{k_3^{(n+3)}}+\frac{\left(1-\sqrt{3}k_1\right)^2(1+z)^{(n+3)}}{k_3^{(n+3)}}+\frac{kk_3^{nk_{11}}}{k_5^2(1+z)^{nk_{11}}}+\frac{3(n-3)(1+z)^{(n+3)}}{k_3^{(n+3)}}+\frac{k(1+z)^{(4-\sqrt{3}k_1+n)}}{k_5^2k_3^{(4-\sqrt{3}k_1+n)}}+\frac{k_{12}(1+z)^{(n+3)}}{k_3^{(n+3)}}\right]$$

43)

$$\rho(z)-p_t(z)=\frac{k_9}{8\pi}\left[\frac{3k_{10}(1+z)^{(n+3)}}{k_3^{(n+3)}}+\frac{\left(1-\sqrt{3}k_1\right)^2(1+z)^{(n+3)}}{k_3^{(n+3)}}+\frac{kk_3^{nk_{11}}}{k_5^2(1+z)^{nk_{11}}}+\frac{3(n-3)(1+z)^{(n+3)}}{k_3^{(n+3)}}+\frac{k_{13}(1+z)^{(n+3)}}{k_3^{(n+3)}}+\frac{k_{14}(1+z)^{(n+3)}}{k_3^{(n+3)}}\right]$$

(44)

$$\rho(z)+3p_r(z)=\frac{k_9}{2\pi}\left[\frac{\left(1-\sqrt{3}k_1\right)^2(1+z)^{(n+3)}}{k_3^{(n+3)}}+\frac{kk_3^{nk_{11}}}{k_5^2(1+z)^{nk_{11}}}-\frac{\omega(n-3)^2(1+z)^{(n+3)}}{k_3^{(n+3)}}+\frac{3(n-3)(1+z)^{(n+3)}}{k_3^{(n+3)}}-\frac{k(1+z)^{(4-\sqrt{3}k_1+n)}}{k_5^2k_3^{(4-\sqrt{3}k_1+n)}}-\frac{k_{12}(1+z)^{(n+3)}}{k_3^{(n+3)}}\right]$$

(45)

$$\rho(z)+3p_t(z)=\frac{k_9}{2\pi}\left[\frac{k_{10}(1+z)^{(n+3)}}{k_3^{(n+3)}}+\frac{\left(1-\sqrt{3}k_1\right)^2(1+z)^{(n+3)}}{k_3^{(n+3)}}+\frac{kk_3^{nk_{11}}}{k_5^2(1+z)^{nk_{11}}}-\frac{\omega(n-3)^2(1+z)^{(n+3)}}{k_3^{(n+3)}}+\frac{3(n-3)(1+z)^{(n+3)}}{k_3^{(n+3)}}-\frac{k_{13}(1+z)^{(n+3)}}{k_3^{(n+3)}}-\frac{k_{14}(1+z)^{(n+3)}}{k_3^{(n+3)}}\right]$$

(46)

Om diagnostics

Om diagnostics is yet another effective instrument that has emerged from the Hubble parameter. It offers the null test for the $\Lambda-CDM$ model. The variance of diagnostic in slope makes it sufficient for refining a variety of DE models extracted from $\Lambda-CDM$. For the flat universe, the om diagnostics (Arora et. al. 2020) is obtained as

$$om(z)=\frac{\left(\frac{H_z}{H_0}\right)^2-1}{(1+z)^3-1}=\frac{(1+z)^{2n}-k_3^{2n}H_0^2}{\left[(1+z)^3-1\right]k_3^{2n}H_0^2}$$

(47)

CONCLUSION:

In this paper, we have considered Ruban space time anisotropic cosmological model in Brans-Dicke scalar-tensor theory of gravitation with an anisotropic dark matter fluid. For solving the field equations, we used the law of Hubble parameter, we use the relation between expansions scalar θ and shear scalar σ . We found metric potential, radial pressure, transverse pressure, anisotropic factor and energy density in terms of redshift. The values of all quantities are depends upon the values of constant, for particular values of constants radial pressure, transverse pressure, anisotropic factor and energy densities are positive. Graphically, we observe that from fig.1 shows that deceleration parameter q is in the range (-1, 0) hence the model represents accelerated expansion of the universe. From fig.2 it is observed that both expansion scalar and shear scalar increases as redshift increases, whereas when redshift is zero the expansion scalar and shear scalars are finite. Using different aspects we discuss the stability of the obtained cosmological model. From figures 6 and 7, it is observed that radial and tangential sound speeds are positive, i.e. $v_r^2>0$ and $v_t^2>0$ it gives stable cosmological model. In addition to the positivity of v_r^2 and v_t^2, the causality condition states that speed of sound is less than speed of light. In the given cosmological model speed of sound is greater than one but speed of sound is not less than speed of light, i.e. it does not lie between 0 and 1. So, for obtained cosmological model the causality condition is not satisfied. Also, stability factor $\left(v_t^2-v_r^2\right)$ for an anisotropic fluid model, from fig. (8), it is clear that stability factor $\left(v_t^2-v_r^2\right)$ lies between -1 and 0. So the model is potentially stable. Also, we obtained different energy conditions and it is observed that all the mentioned energy conditions are satisfied. We have also obtained the Om diagnostics were a useful test for comparing the model to the conventional ΛCDM model. Also it is observed that best-fitted curve closely matched the data points when we compared the the graph of the Hubble parameter with the Hubble dataset, the graph illustrates the history of the expansion of the universe, which is characterized by an increase in the Hubble parameter as redshift increases. This increase

http://doi.org/10.29369/ijrbat.2025.010.2.00012

reflects the evolution from an early universe dominated by radiation to an age dominated by matter and then eventually to a dark energy-dominated, accelerating expansion phase.

REFERENCE:

Brans, C., & Dicke, R. H. (1961). Mach's principle and a relativistic theory of gravitation. *Physical review*, *124*(3), 925.

Clifton, T., Ferreira, P. G., Padilla, A., & Skordis, C. (2012). Modified gravity and cosmology. *Physics reports*, *513*(1-3), 1-189.

Ahmadi-Azar, E., Atazadeh, K., & Eghbali, A. (2024). Linear independence of field equations in the Brans-Dicke theory. *arXiv preprint arXiv:2410.13316*.

MISHRA, R. K., & Sharma, R. (2024). Investigating the Bianchi IX universe within Brans Dicke theory & a novel deceleration parameter.

Sharma, M., Vicente, G. S., Graef, L. L., Ramos, R. O., & Wang, A. (2025). Quantum geometric formulation of Brans-Dicke theory for Bianchi I spacetime. *Physical Review D*, *111*(4), 043501.

Santhi, M. V., & SantoshRupa, K. (2024). Study on Anisotropic Dark Energy Cosmological Models in Generalized Brans-Dicke Theory. *East European Journal of Physics*, (3), 103-115.

Satyanarayana, P. E., & Sireesha, K. V. S. (2024). Bianchi Type-III Viscous Holographic Ricci Dark energy Cosmological model in Brans-Dicke theory of Gravitation. *East European Journal of Physics*, (1), 127-135.

Çağlar, H. (2023). An investigation into lrs bianchi i universe in brans-dicke theory. *Journal of New Theory*, (44), 87-96.

Bamba, K., Bhatti, M. Z., Yousaf, Z., & Shoukat, Z. (2023). Gravitational decoupling of anisotropic stars in the Brans–Dicke theory. *The European Physical Journal C*, *83*(11), 1033.

Santhi, M. V., Chinnappalanaidu, T., Madhu, S. S., & Gusu, D. M. (2022). Some Bianchi type viscous holographic dark energy cosmological models in the Brans–Dicke theory. *Advances in Astronomy*, *2022*(1), 5364541.

Bhardwaj, V. K., Dixit, A., & Pradhan, A. (2023). Bianchi type-V transitioning model in Brans–Dicke theory with observational constraints. *International Journal of Geometric Methods in Modern Physics*, *20*(02), 2350022.

Kapse, D. V., & Katore, S. D. (2022). Evolution of Viscous Dark Energy Models in Brans-Dicke Theory of Gravitation. *Bulgarian Journal of Physics*, *49*(4).

Roy, S. (2021) A Simple Way to Estimate the Variation of the Gravitational Constant as a Function of Redshift in the Framework of Brans-Dicke Theory. *rn*, *55*, 7.

Singh, S. S., & Soibam, Y. (2021). Anisotropic models with generalized hybrid expansion in Brans–Dicke theory of gravity. *International Journal of Geometric Methods in Modern Physics*, *18*(09), 2150141.

Shaikh, A. Y. (2020). Viscous Dark Energy Cosmological Models in Brans-Dicke Theory of Gravitation. *Bulgarian Journal of Physics*, *47*.

Aditya, Y., Mandal, S., Sahoo, P. K., & Reddy, D. R. K. (2019). Observational constraint on interacting Tsallis holographic dark energy in logarithmic Brans–Dicke theory. *The European Physical Journal C*, *79*(12), 1020.

Pawar, D. D., Shahare, S. P., & Dagwal, V. J. (2018). Tilted Kantowski–Sachs cosmological model in Brans–Dicke theory of gravitation. *Modern Physics Letters A*, *33*(04), 1850011.

Tirandari, M., & Saaidi, K. (2017). Anisotropic inflation in Brans–Dicke gravity. *Nuclear Physics B*, *925*, 403-414.

Biswas, R., & Debnath, U. (2014). Constraining red-shift parametrization parameters in Brans-Dicke theory: evolution of open confidence contours. *Astrophysics and Space Science*, *353*, 721-730.

Pawar, D. D., & Solanke, Y. S. (2014). Exact kantowski-sachs anisotropic dark energy cosmological models in brans dicke theory of gravitation. *International Journal of Theoretical Physics*, *53*, 3052-3065.

Avilez, A., & Skordis, C. (2014). Cosmological constraints on Brans-Dicke theory. *Physical review letters*, *113*(1), 011101.

Vidyasagar, T., Naidu, R. L., Bhuvana Vijaya, R., & Reddy, D. R. K. (2014). Bianchi type-VI 0 bulk viscous string cosmological model in Brans-Dicke scalar-tensor theory of gravitation. *The European Physical Journal Plus*, *129*, 1-7.

Vidyasagar, T., Naidu, R. L., Bhuvana Vijaya, R., & Reddy, D. R. K. (2014). Bianchi type-VI 0 bulk viscous string cosmological model in Brans-Dicke scalar-tensor theory of gravitation. *The European Physical Journal Plus*, *129*, 1-7.

Reddy, D. R. K., & Vijaya Lakshmi, G. V. (2014). Five dimensional radiating model in Brans-Dicke theory of gravitation. *Astrophysics and Space Science*, *354*, 633-636

Adhav, K. S., Nimkar, A. S., Ugale, M. R., & Dawande, M. V. (2008). Bianchi Type-III cosmological model with negative constant deceleration parameter in Brans Dicke theory

http://doi.org/10.29369/ijrbat.2025.010.2.00012

of gravitation. *International Journal of Theoretical Physics*, *47*, 634-639.

Lima, J. A. S., & Nobre, M. A. S. (1990). Inhomogeneous two-fluid cosmologies with electromagnetic field. *Classical and Quantum Gravity*, *7*(3), 399.

Lima, J. A. S., & Tiomno, J. (1988). Inhomogeneous two-fluid cosmologies. *General relativity and gravitation*, *20*, 1019-1035.

Tomimura, N., & Waga, I. (1987). Inhomogeneous cosmological models-New exact solutions with dust, isotropic radiation, and electromagnetic field. *Astrophysical Journal, Part 1 (ISSN 0004-637X), vol. 317, June 1, 1987, p. 52-61.*, *317*, 52-61.

wath,J.S., Nimkar, A.S.(2024). Stability of Microscopic body cosmological model in Ruban's background Jnanabha, Vol. 54(1) (2024), 1-9

Aktaş, C. (2019). Energy–momentum distributions of Ruban universe in general relativity and teleparallel gravity. *International Journal of Modern Physics A*, *34*(03n04), 1950011.

Mete, V. G., Elkar, V. D., & Nimkar, A. S. (2015). Ruban's Cosmological Modelwith Bulk Stress In General Theory of Relativity. *IOSR J. Math.*, *11*, 25-33.

Ugale, M. R., & Deshmukh, S. B. (2024). Anisotropic bianchi type VI 0 cosmological models in a modified f (R, T) gravity. *Journal of Scientific Research*, *16*(1), 17-30.

Dhore, A. O., & Ugale, M. R. (2024). Study of f (T) Theory of Gravity in the Framework of Modified Holographic Ricci Dark Energy with Thermodynamical Aspects. *International Journal of Theoretical Physics*, *63*(8), 202.

Sarkar, N., Sarkar, S., Singh, K. N., & Rahaman, F. (2020). Relativistic compact stars with dark matter density profile. *The European Physical Journal C*, *80*(3), 255.

Bhar, P., Singh, K. N., Sarkar, N., & Rahaman, F. (2017). A comparative study on generalized model of anisotropic compact star satisfying the Karmarkar condition. *The European Physical Journal C*, *77*(9), 596.

Wath, J. S., & Nimkar, A. S. (2024). Anisotropic dark matter distribution in Saez–Ballester theory of gravitation. *Indian Journal of Physics*, *98*(8), 3011-3017.

Wath, J. S., & Nimkar, A. S. (2023). Cosmological Parameters and Stability of Bianchi Type-VIII in Sáez-Ballester Theory of Gravitation. *Bulgarian Journal of Physics*, *50*(3).

Thirukkanesh, S., Bogadi, R. S., Govender, M., & Moyo, S. (2021). Stability and improved physical characteristics of relativistic compact objects arising from the quadratic term in p_r= α ρ^ 2+ β ρ-γ pr= α ρ 2+ β ρ-γ. *The European Physical Journal C*, *81*, 1-7.

Herrera, L. (2020). Stability of the isotropic pressure condition. *Physical Review D*, *101*(10), 104024.

Ahmed, N., & Alamri, S. Z. (2018). A stable flat universe with variable cosmological constant in f (R, T) gravity. *Research in Astronomy and Astrophysics*, *18*(10), 123.

Franco, G. A. R., Escamilla-Rivera, C., & Levi Said, J. (2020). Stability analysis for cosmological models in f (T, B) gravity. *The European Physical Journal C*, *80*(7), 677.

Knutsen, H. (1988). Some physical properties and stability of an exact model of a relativistic star. *Astrophysics and space science*, *140*, 385-401.

Knutsen, H. (1988). On the stability and physical properties of an exact relativistic model for a superdense star. *Monthly Notices of the Royal Astronomical Society*, *232*(1), 163-174.

Wanas, M. I., & Bakry, M. A. (1995). Stability of cosmological models. *Astrophysics and Space Science*, *228*, 239-253.

Rahaman, F., Ray, S., Jafry, A. K., & Chakraborty, K. (2010). Singularity-free solutions for anisotropic charged fluids with Chaplygin equation of state. *Physical Review D—Particles, Fields, Gravitation, and Cosmology*, *82*(10), 104055.

Kiran, M., Reddy, D. R. K., & Rao, V. U. M. (2015). Minimally interacting holographic Dark energy model in Brans-Dicke theory. *Astrophysics and Space Science*, *356*, 407-411.

Akarsu, Ö., & Dereli, T. (2012). Cosmological models with linearly varying deceleration parameter. *International Journal of Theoretical Physics*, *51*, 612-621.

Berman, M. S. (1983). A special law of variation for Hubble's parameter. *Nuovo Cimento B Serie*, *74*, 182-186.

Berman, M. S., & de Mello Gomide, F. (1988). Cosmological models with constant deceleration parameter. *General Relativity and Gravitation*, *20*, 191-198.

Pawar, D.D., Gaikwad, P. S. & Ghungarwar N.G. (2023) Two Fluids in F(T) Gravity with Observational Constraints, *Astronomy and Computing*, *48*, 100863.

Abreu, H., Hernández, H., & Núnez, L. A. (2007). Sound speeds, cracking and the stability of self-gravitating anisotropic compact

http://doi.org/10.29369/ijrbat.2025.010.2.00012

objects. *Classical and Quantum Gravity*, *24*(18), 4631.

Sharov, G. S., & Vasiliev, V. O. (2018). How predictions of cosmological models depend on Hubble parameter data sets. *arXiv preprint arXiv:1807.07323*.

Arora, S., Pacif, S. K. J., Bhattacharjee, S., & Sahoo, P. K. (2020). f (Q, T) gravity models with observational constraints. *Physics of the Dark Universe*, *30*, 100664.

Stern, D., Jimenez, R., Verde, L., Kamionkowski, M., & Stanford, S. A. (2010). Cosmic chronometers: constraining the equation of state of dark energy. I: H (z) measurements. *Journal of Cosmology and Astroparticle Physics*, *2010*(02), 008.

Simon, J., Verde, L., & Jimenez, R. (2005). Constraints on the redshift dependence of the dark energy potential. *Physical Review D—Particles, Fields, Gravitation, and Cosmology*, *71*(12), 123001.

Moresco, M., Cimatti, A., Jimenez, R., Pozzetti, L., Zamorani, G., Bolzonella, M., ... & Welikala, N. (2012). Improved constraints on the expansion rate of the Universe up to z~ 1.1 from the spectroscopic evolution of cosmic chronometers. *Journal of Cosmology and Astroparticle Physics*, *2012*(08), 006.

Zhang, C., Zhang, H., Yuan, S., Liu, S., Zhang, T. J., & Sun, Y. C. (2014). Four new observational H (z) data from luminous red galaxies in the Sloan Digital Sky Survey data release seven. *Research in Astronomy and Astrophysics*, *14*(10), 1221.

Moresco, M., Pozzetti, L., Cimatti, A., Jimenez, R., Maraston, C., Verde, L., ... & Wilkinson, D. (2016). A 6% measurement of the Hubble parameter at z~ 0.45: direct evidence of the epoch of cosmic re-acceleration. *Journal of Cosmology and Astroparticle Physics*, *2016*(05), 014.

Ratsimbazafy, A. L., Loubser, S. I., Crawford, S. M., Cress, C. M., Bassett, B. A., Nichol, R. C., & Väisänen, P. (2017). Age-dating luminous red galaxies observed with the Southern African Large Telescope. *Monthly Notices of the Royal Astronomical Society*, *467*(3), 3239-3254.

Moresco, M. (2015). Raising the bar: new constraints on the Hubble parameter with cosmic chronometers at z~ 2. *Monthly Notices of the Royal Astronomical Society: Letters*, *450*(1), L16-L20.

Gaztanaga, E., Cabre, A., & Hui, L. (2009). Clustering of luminous red galaxies–IV. Baryon acoustic peak in the line-of-sight direction and a direct measurement of H (z). *Monthly Notices of the Royal Astronomical Society*, *399*(3), 1663-1680.

Oka, A., Saito, S., Nishimichi, T., Taruya, A., & Yamamoto, K. (2014). Simultaneous constraints on the growth of structure and cosmic expansion from the multipole power spectra of the SDSS DR7 LRG sample. *Monthly Notices of the Royal Astronomical Society*, *439*(3), 2515-2530.

Wang, Y., Zhao, G. B., Chuang, C. H., Ross, A. J., Percival, W. J., Gil-Marín, H., ... & Zhu, F. (2017). The clustering of galaxies in the completed SDSS-III Baryon Oscillation Spectroscopic Survey: tomographic BAO analysis of DR12 combined sample in configuration space. *Monthly Notices of the Royal Astronomical Society*, *469*(3), 3762-3774.

Chuang, C. H., Prada, F., Pellejero-Ibanez, M., Beutler, F., Cuesta, A. J., Eisenstein, D. J., ... & Thomas, D. (2016). The clustering of galaxies in the SDSS-III Baryon Oscillation Spectroscopic Survey: single-probe measurements from CMASS anisotropic galaxy clustering. *Monthly Notices of the Royal Astronomical Society*, *461*(4), 3781-3793.

Alam, S., Ata, M., Bailey, S., Beutler, F., Bizyaev, D., Blazek, J. A., ... & Zhao, G. B. (2017). The clustering of galaxies in the completed SDSS-III Baryon Oscillation Spectroscopic Survey: cosmological analysis of the DR12 galaxy sample. *Monthly Notices of the Royal Astronomical Society*, *470*(3), 2617-2652.

Blake, C., Brough, S., Colless, M., Contreras, C., Couch, W., Croom, S., ... & Yee, H. K. (2012). The WiggleZ Dark Energy Survey: Joint measurements of the expansion and growth history at z< 1. *Monthly Notices of the Royal Astronomical Society*, *425*(1), 405-414.

Chuang, C. H., Prada, F., Cuesta, A. J., Eisenstein, D. J., Kazin, E., Padmanabhan, N., ... & Thomas, D. (2013). The clustering of galaxies in the SDSS-III Baryon Oscillation Spectroscopic Survey: single-probe measurements and the strong power of f (z) σ8 (z) on constraining dark energy. *Monthly Notices of the Royal Astronomical Society*, *433*(4), 3559-3571.

Anderson, L., Aubourg, E., Bailey, S., Beutler, F., Bhardwaj, V., Blanton, M., ... & Zhao, G. B. (2014). The clustering of galaxies in the SDSS-III Baryon Oscillation Spectroscopic Survey: baryon acoustic oscillations in the Data Releases 10 and 11 Galaxy samples. *Monthly Notices of the Royal Astronomical Society*, *441*(1), 24-62.

http://doi.org/10.29369/ijrbat.2025.010.2.00012

Busca. N. G, Delubac T., Rich J.,et al. "Baryon Acoustic Oscillations in the Ly- α forest of BOSS quasars," arXiv preprint arXiv preprint arXiv:1211.2616 (2012).

Bautista, J. E., Guy, J., Rich, J., Blomqvist, M., Des Bourboux, H. D. M., Pieri, M. M., ... & Yèche, C. (2017). Measurement of baryon acoustic oscillation correlations at z= 2.3 with SDSS DR12 Lyα-Forests. *Astronomy & Astrophysics*, *603*, A12.

Delubac, T., Rich, J., Bailey, S., Font-Ribera, A., Kirkby, D., Le Goff, J. M., ... & York, D. G. (2013). Baryon acoustic oscillations in the Lyα forest of BOSS quasars. *Astronomy & Astrophysics*, *552*, A96.

Font-Ribera, A., Kirkby, D., Miralda-Escudé, J., Ross, N. P., Slosar, A., Rich, J., ... & York, D. G. (2014). Quasar-Lyman α forest cross-correlation from BOSS DR11: Baryon Acoustic Oscillations. *Journal of Cosmology and Astroparticle Physics*, *2014*(05), 027.

http://doi.org/10.29369/ijrbat.2025.010.2.00012